View Article Online / Journal Homepage / Table of Contents for this issue
Dynamic Article Links

PCCP

Cite this: *Phys. Chem. Chem. Phys.*, 2011, **13**, 4303–4310

www.rsc.org/pccp

PAPER

A superfluorescent fluorenyl probe with efficient two-photon absorption

Kevin D. Belfield,*[ab] Mykhailo V. Bondar,[c] Florencio E. Hernandez,[ab] Olga V. Przhonska,[c] Xuhua Wang[a] and Sheng Yao[a]

Received 16th August 2010, Accepted 21st December 2010
DOI: 10.1039/c0cp01511c

Published on 21 January 2011 on http://pubs.rsc.org | doi:10.1039/C0CP01511C
Downloaded by University of Central Florida on 17 December 2012

The linear photophysical, excited state absorption (ESA), superfluorescence, and two-photon absorption (2PA) properties of 4,4′-(1*E*,1′*E*)-2,2′-(7,7′(1*E*,1′*E*)2,2′(4,4′-sulfonylbis(4,1-phenylene))-bis(ethane-2,1-diyl)bis(9,9-didecy-9*H*-fluorene7,2-diyl))bis(ethane-2,1-diyl)bis(*N*,*N*-diphenylaniline) (**1**) were investigated in organic and aqueous media with respect to its potential application in biological imaging. The analysis of linear photophysical properties revealed a rather complex nature of the main one-photon absorption band, strong solvatochromic effects in the steady-state fluorescence spectra, single-exponential fluorescence decay, and high fluorescence quantum yields in organic solvents ($\approx$1.0). The ESA spectra of **1** suggested potential for light amplification in nonpolar media while efficient superfluorescence in cyclohexane was demonstrated. The degenerate 2PA spectra of **1** were obtained over a broad spectral range (640–900 nm), using a standard two-photon induced fluorescence method under 1 kHz femtosecond excitation. Two well defined 2PA bands with maximum 2PA cross sections up to 1700 GM in the higher energy, short wavelength band and $\approx$1200 GM in the lower energy, long wavelength band of **1** were shown. The potential use of **1** in bioimaging was demonstrated *via* one- and two-photon *in vitro* fluorescence imaging of HCT 116 cells.

1. Introduction

The synthesis and photophysical investigation of new organic molecules with large two-photon absorption (2PA) cross sections is promising for the development of nonlinear optical materials.[1] Among the vast diversity of 2PA chromophores systems, fluorene derivatives with extended π-conjugation are among the best candidates for a number of important applications, such as two-photon fluorescence microscopy (2PFM),[2,3] 3D microfabrication[4] and optical data storage,[5] upconverted lasing,[6] optical power limiting,[7] and two-photon photodynamic therapy.[3,8] The main principles of the design and synthesis of fluorene-based compounds with efficient 2PA are sufficiently well established and described previously.[9] The molecular structure should consist of electron-donating or electron-withdrawing moieties, arranged in a symmetrical or nonsymmetrical fashion with extended π-conjugation (large number of polarizable π-electrons).[10] In the case of two or more chromophore systems in the same molecular structure, an additional specific effect on 2PA efficiency in the main one-photon absorption band can be expected due to intramolecular interaction of these chromophores.[11]

In this paper, the linear photophysical, excited state absorption (ESA), superfluorescence, and 2PA properties of a double fluorenyl chromophore derivative, 4,4′-(1*E*,1′*E*)-2,2′-(7,7′-(1*E*,1′*E*)2,2′(4,4′-sulfonylbis(4,1-phenylene))bis(ethene-2,1-diyl)-bis(9,9-didecy-9*H*-fluorene-7,2-diyl))bis(ethane-2,1-diyl)bis(*N*,*N*-diphenylaniline) (**1**), were investigated as a promising fluorescence probe for two-photon bioimaging applications. A comprehensive analysis of the nature of the fluorescence and linear absorption bands of **1** was performed by time-resolved emission and excitation anisotropy methods.[12] The values of 2PA cross sections, δ_{2PA}, were determined over a broad spectral range *via* two-photon induced fluorescence (2PF) methodology[13] under 1 kHz femtosecond excitation. ESA and superfluorescence properties of **1** were investigated as a first step in the development of a new class of superfluorescent probes possessing short luminescence lifetimes and increased spectral brightness, which can dramatically improve the quality of biological fluorescent images. The potential ability of fluorenyl probe **1** in bioimaging was demonstrated *via* one- and two-photon fluorescence imaging of HCT 116 cells after incubation with **1**.

2. Experimental section

2.1 Linear photophysical measurements

The molecular structure of fluorenyl probe **1** is presented in Fig. 1. The synthesis of **1** was recently reported.[14] All linear

[a] *Department of Chemistry, University of Central Florida, P.O. Box 162366, Orlando, FL 32816-2366, USA. E-mail: belfield@mail.ucf.edu*
[b] *CREOL, The College of Optics and Photonics, University of Central Florida, P.O. Box 162366, Orlando, FL 32816-2366, USA*
[c] *Institute of Physics, Prospect Nauki, 46, Kiev-28, 03028, Ukraine*

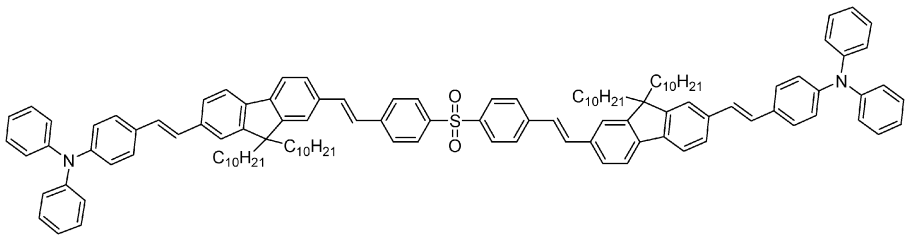

Fig. 1 Molecular structure of **1**.

Published on 21 January 2011 on http://pubs.rsc.org | doi:10.1039/C0CP01511C
Downloaded by University of Central Florida on 17 December 2012

photophysical parameters were measured in spectroscopic grade hexane, cyclohexane, toluene, tetrahydrofuran (THF), dichloromethane (DCM) and an aqueous solution (95 wt% water/5 wt% DMSO). Linear (one-photon) absorption spectra of **1** were determined with an Agilent 8453 UV–visible spectrophotometer for a broad range of molecular concentrations, 2×10^{-2} M $\leq C \leq 10^{-6}$ M, using quartz cuvettes with different path lengths (0.01, 0.1, 1.0, and 10 mm). The steady-state fluorescence and excitation anisotropy spectra of **1** were measured with a PTI QuantaMaster spectrofluorimeter in the photon counting regime, in 10 mm spectrofluorometric quartz cuvettes for dilute solutions, $C \leq 10^{-6}$ M. The fluorescence spectra were corrected for the spectral responsivity of the PTI emission monochromator and PMT detection system. The excitation anisotropy spectra of **1** were obtained using an L-format configuration,[12] while weak emission of pure solvent and scattered light were extracted. The values of fundamental anisotropy, r_0, were determined at room temperature in viscous poly(tetrahydrofuran) (pTHF), where the rotational correlation time, $\theta \gg \tau$ (τ is the fluorescence lifetime of **1**) and observed anisotropy $r = r_0/(1 + \theta/\tau) \approx r_0$.[12] Fluorescence quantum yields, Φ, were obtained in dilute solutions by a standard method relative to 9,10-diphenylanthracene in cyclohexane ($\Phi \approx 0.95$) as a reference.[12] Concentration dependences $\Phi = f(C)$ were determined using 0.1 mm quartz cuvettes under the front face excitation geometry.[15] The values of fluorescence lifetimes of **1** were obtained with a time-correlated single photon counting system, PicoHarp 300, under 76 MHz femtosecond laser excitation (Mira 900, Coherent) with time resolution $\approx$ 80 ps. Linear polarization of the laser beam was oriented by the magic angle to avoid a possible effect of molecular rotation on fluorescence kinetics.

2.2 Two-photon spectral and bioimaging measurements

The degenerate 2PA spectra of **1** were measured in nonpolar solvent (cyclohexane) and polar solvent (DCM) over a broad spectral region by a typical 2PF method[13] relative to Rhodamine B in methanol as a standard.[16] The 2PF method was used with a PTI QuantaMaster spectrofluorimeter coupled to a femtosecond Clark-MXR CPA-2010 laser pumped optical parametric generator/amplifier (TOPAS) with tuning range 600–950 nm, pulse duration $\approx$ 140 fs (FWHM), 1 kHz repetition rate, and pulse energies $E_P \leq 0.15$ μJ. Two-photon fluorescence measurements were performed in the analog regime of the PMT, using 10 mm fluorometric quartz cuvettes with dye concentration $\sim 10^{-5}$ M. The 2PA cross sections, δ_{2PA}, were determined by the equation:[13]

$$\delta^{S}_{2PA} = \delta^{R}_{2PA} \cdot \frac{\langle F(t)\rangle_S \cdot C_R \cdot \Phi_R \cdot \varphi_R \cdot \langle P(t)\rangle^2_R}{\langle F(t)\rangle_R \cdot C_S \cdot \Phi_S \cdot \varphi_S \cdot \langle P(t)\rangle^2_S},$$

where $\langle F(t)\rangle$, $\langle P(t)\rangle$, C, and φ are the averaged fluorescence intensity, excitation power, molecular concentration, and geometric factor, respectively. Subscripts S and R correspond to the sample and reference compound. The quadratic dependence of 2PF intensity on the excitation power was verified for each excitation wavelength, λ_{ex}, while no spectral dependence $\Phi = f(\lambda_{ex})$ was observed for all solvents utilized in the 2PA measurements.

For two-photon fluorescence imaging, HCT 116 cells were placed onto poly-D-lysine coated glass coverslips in 24-well plates (40 000 cells per well), and the cells were incubated for 36 h before incubating with a fluorescent probe. A stock solution (0.5 mM) of the fluorescent probe in Pluronic F 108NF micelles was dissolved in water. The stock solution of fluorophore encapsulated micelles was prepared by mixing a solution of dye in DCM (5 mL) with Pluronic F 108NF (30 mg) in water (5 mL), followed by slow evaporation of DCM at room temperature over 48 h with stirring. The dye concentration was approximately 0.5 mM in water as estimated by absorption spectra. Diluted 30 μM solutions of dye in complete growth medium, Dulbecco's modification of Eagle's medium (DMEM), were then freshly prepared and placed over the cells for a 3 h period. After incubation, the cells were washed with PBS (3–5×) and fixed using 3.7% formaldehyde solution for 15 min at 37 °C. Then 0.5 mL per well $NaBH_4$ (1 mg mL^{-1}) solution in PBS (pH = 8.0), which was prepared by adding few drops of 6 N NaOH solution into PBS (pH = 7.2), was placed in each well for 15 min and repeated once. Then the plates were washed twice with PBS and once with water. Finally, the glass coverslips were mounted with Prolong Gold mounting media for microscopy.

An inverted microscope (Olympus IX70) equipped with a Q Imaging cooled CCD (Model Retiga EXi) was used for conventional fluorescence imaging, where the output of a filtered 100 W mercury lamp was used as the excitation source. A customized filter cube (Ex 377/50, DM 409, Em 460/50) was used for fluorescence imaging.

Two-photon fluorescence microscopy (2PFM) images were collected on a modified Olympus Fluoview FV300 microscope system coupled to a tunable Coherent Mira 900F Ti:sapphire, 76 MHz, modelocked, femtosecond laser tuned to 700 nm. The two-photon induced fluorescence was collected with a

 This journal is © the Owner Societies 2011

Published on 21 January 2011 on http://pubs.rsc.org | doi:10.1039/C0CP01511C
Downloaded by University of Central Florida on 17 December 2012

60× microscope objective (UPLANSAPO 60×, NA = 1.35, Olympus). A long-pass emission filter (cutoff 690 nm) was placed in the microscope scanhead to avoid background light from the excitation source. Consecutive layers, separated by approximately 0.3 μm, were recorded to create a 3D reconstruction from overlaid 2PFM images.

2.3 ESA and superfluorescence measurements

The ESA spectra of **1** were obtained in cyclohexane and DCM using a pump–probe technique[17] with a picosecond Nd:YAG laser (PL 2143 B Ekspla). The experimental setup is shown in Fig. 2. A strong pump beam at λ_{ex} = 355 nm, with pulse duration, $\tau_P \approx 35$ ps, (FWHM), pulse energy, $E_P \leq 15$ μJ, and 10 Hz repetition rate, was focused into a 1 mm cuvette with dye concentration $C \sim 10^{-5}$ M. A weak white light continuum (WLC) pulse, generated by the primary laser output (1064 nm) in a 10 cm path length quartz cuvette filled with de-ionized water, was used as a probe beam. Vertically polarized pump and probe beams were spatially overlapped inside the sample, and the probe pulse was delayed by ~100 ps relative to the pump. The changes in the spectral shape of the probe WLC beam induced by the pumped sample medium were measured with a USB-2000 Ocean Optics spectrometer, facilitating determination of the corresponding ESA spectra. Superfluorescence spectra of **1** were measured in cyclohexane, with dye concentration $C \sim 10^{-4}$ M, under longitudinal pumping at 355 nm (Fig. 2, left channel) with pulse energy $E_P \leq 15$ μJ. Solutions of **1** were placed in 4 mm quartz cells. The position of the samples inside the focusing caustic (15 cm lens (Fig. 2, L_1)) was selected to reach the highest efficiency of superfluorescence. Spectral measurements were performed with the same USB-2000 spectrometer. It should be mentioned, that besides superfluorescence, the effect of laser oscillation also was observed in cyclohexane in the direction perpendicular to the exit surfaces of the quartz cells, that served as a resonator, while superfluorescence emission occurred in the direction of the pump beam.

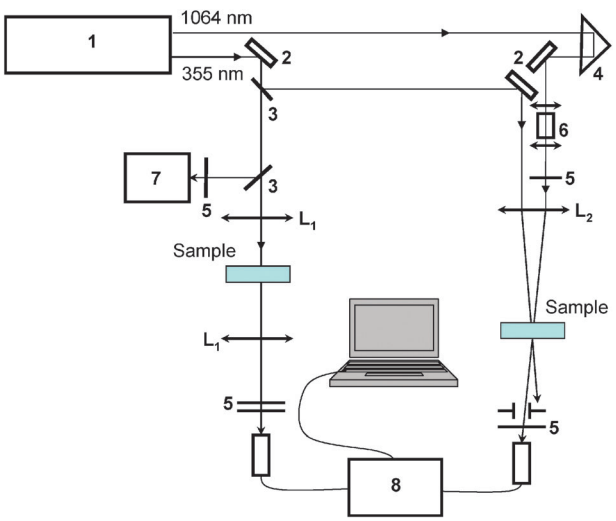

Fig. 2 Experimental setup for ESA and superfluorescence: picosecond laser (1); 100% reflection mirrors (2); beam splitters (3); delay line (4); focusing lens (L_1—15 cm; L_2—25 cm); neutral density and color filters (5); water cell (6); silicon detectors (7); and spectrometer (8).

3. Results and discussion

3.1 Linear spectral properties

Compound **1** is a symmetrical donor–acceptor–donor type molecule with two independent fluorene-based chromophore systems. A quantum chemical calculation of the optimized geometry of **1** by the AM1 method (HyperChem V7.0) indicates a noncollinear intramolecular orientation of these two main chromophores with an ~60° angle between their axes, which can influence fluorescence polarization properties. The steady-state absorption and fluorescence spectra of **1**, along with its other linear photophysical parameters are presented in Fig. 3 and 4, and Table 1, respectively. In organic solvents, the absorption spectra were nearly independent of solvent polarity and their shape and maximum extinction coefficients, ε^{max}, exhibited no dependence on molecular concentration up to $C \approx 2 \times 10^{-2}$ M (Fig. 4a, curve B). This indicates possible aggregation processes in organic solvents were negligible and did not affect the spectral measurements.

The fluorescence spectra of **1** in organic solvents were independent of excitation wavelength, λ_{ex}, and exhibited strong solvatochromic behavior. A simple quantum-chemical analysis of the electronic structure of **1** performed by a semi-empirical ZINDO/S method (HyperChem V7.0) showed relatively small changes in the stationary dipole moment, $|\Delta\mu| < 0.5$ D, under electronic excitation $S_0 \rightarrow S_1$ (S_0 and S_1 are the ground and first excited electronic states, respectively). In this case, the values of large Stokes shifts in polar solvents (see Table 1) did not conform to the Lippert equation[12] and can be explained by symmetry breaking effects in the electronic distribution of **1** that occur in the S_1 excited state due to intramolecular chromophore electronic interactions and/or electron–vibration coupling.[18] Such solvatochromic spectral behavior is typical for symmetrical donor–acceptor fluorenes with extended π-conjugation.[19,20] The fluorescence quantum yields, Φ, were close to 1.0 in organic solvents of varying polarity and independent of concentration (up to $C \approx 2 \times 10^{-2}$ M) and excitation wavelength λ_{ex} over a broad spectral range (Fig. 4a and b). Fluorescence lifetimes, τ, of **1** in

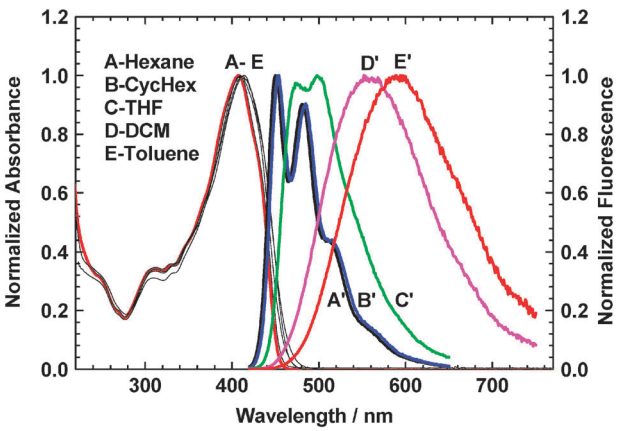

Fig. 3 Normalized one-photon absorption (A–E) and fluorescence (A′–E′) spectra of **1** in hexane (A, A′), cyclohexane (B, B′), toluene (E, C′), THF (C, D′), and DCM (D, E′). Solvents are listed in the order of increasing maximum absorption wavelength of **1**.

Downloaded by University of Central Florida on 17 December 2012
Published on 21 January 2011 on http://pubs.rsc.org | doi:10.1039/C0CP01511C

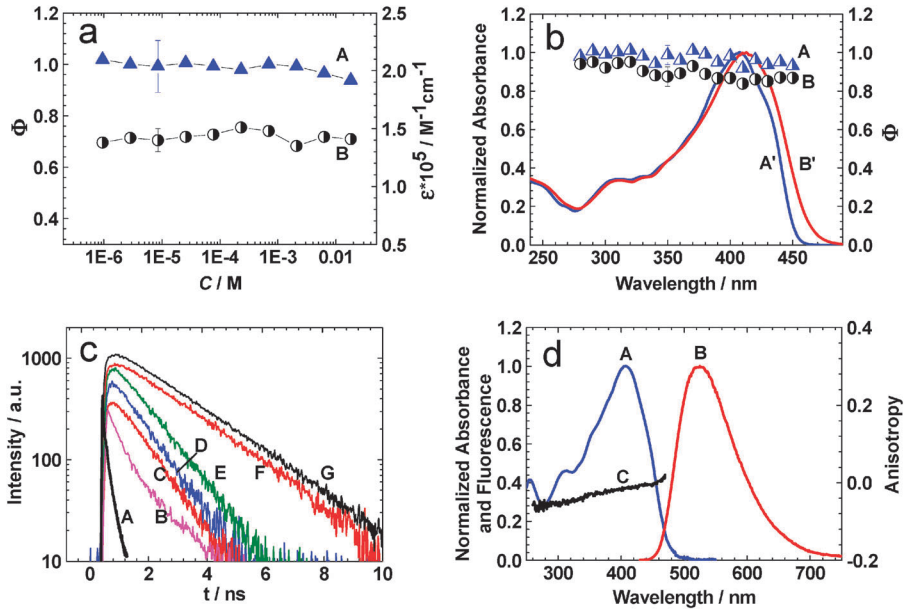

Fig. 4 (a) Concentration dependences of the fluorescence quantum yield $\Phi = f(C)$ (A) and maximum extinction coefficient of $\varepsilon^{max} = f(C)$ (B) of **1** in cyclohexane. (b) Spectral dependences of $\Phi = f(\lambda_{ex})$ (A, B) and normalized one-photon absorption spectra (A′, B′) of **1** in cyclohexane (A, A′) and DCM (B, B′). (c) Fluorescence decays of **1** in hexane (C), cyclohexane (D), toluene (E), THF (F), DCM (G), aqueous, 95 wt% water/5 wt% DMSO, solution (B), and Instrument Response Function (A). (d) Normalized absorption (A), fluorescence (B), and anisotropy (C) spectra of **1** in aqueous, 95 wt% water/5 wt% DMSO, solution.

Table 1 Linear photophysical parameters of **1** in different solvents: absorption λ_{abs}^{max} and fluorescence λ_{fl}^{max} maxima, Stokes shifts, maximum extinction coefficients ε^{max}, fluorescence quantum yields Φ and lifetimes τ

N/N	Hexane	Cyclohexane	Toluene	THF	DCM	Aqueous mixture[a]
λ_{abs}^{max}/nm	408 ± 1	408 ± 1	413 ± 1	409 ± 1	412 ± 1	407 ± 1
λ_{fl}^{max}/nm	450 ± 1	453 ± 1	499 ± 1	558 ± 1	590 ± 1	523 ± 1
Stokes shift/nm	42 ± 2	45 ± 2	86 ± 2	149 ± 2	178 ± 2	116 ± 2
ε^{max} 10^{-3}/M^{-1} cm^{-1}	135 ± 15	145 ± 10	135 ± 10	145 ± 10	130 ± 10	—
Φ	1.0 ± 0.05	1.0 ± 0.05	1.0 ± 0.05	1.0 ± 0.05	0.92 ± 0.07	0.40 ± 0.05
τ^{b}/ns	1.1 ± 0.05	1.1 ± 0.05	1.2 ± 0.05	2.35 ± 0.05	2.33 ± 0.05	0.47 ± 0.05 1.87 ± 0.05

[a] 95 wt% water/5 wt% DMSO. [b] All lifetime measurements correspond to goodness-of-fit parameter $\chi^2 \geq 0.99$.

organic solvents corresponded to a single-exponential decay (Fig. 4c, curves C–G), exhibiting a pronounced increase with solvent polarity (see Table 1).

In an aqueous medium (95 wt% water/5 wt% DMSO), fluorene **1** exhibited complex inhomogeneous broadening of linear spectral properties (Fig. 4d), including a strong dependence of the fluorescence spectra on λ_{ex}, bi-exponential fluorescence decay (Fig. 4c, curve B) with the major component ≈ 0.47 ns (amplitude ~ 85%), decreased quantum yield ($\Phi \sim 0.4$), and close to zero excitation anisotropy (Fig. 4d, curve C), representing several types of solvated molecules (two main types) with different spectral and lifetime properties.

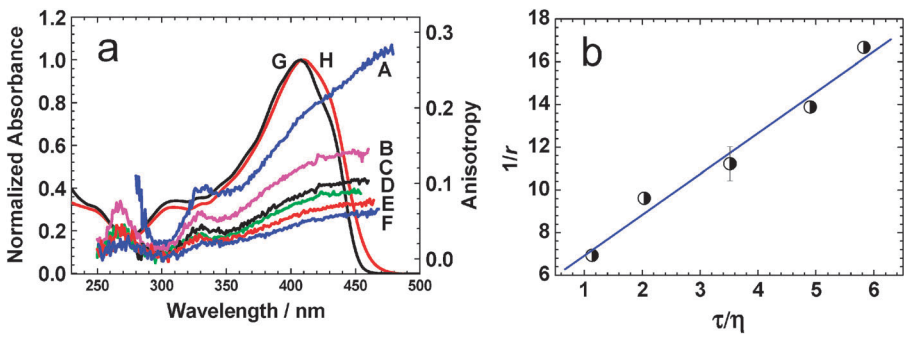

Fig. 5 (a) Excitation anisotropy (A–F) and normalized one-photon absorption spectra (G, H) of **1** in pTHF (A), hexane (D, G), cyclohexane (B), toluene (C), THF (E, H), and DCM (F). (b) Experimental dependence $1/r(\lambda_{ex}) = f(1/\eta)$ for **1** in organic media (solid line is the linear fit).

 This journal is © the Owner Societies 2011

Published on 21 January 2011 on http://pubs.rsc.org | doi:10.1039/C0CP01511C
Downloaded by University of Central Florida on 17 December 2012

The steady-state excitation anisotropy spectra of **1** (Fig. 5a) provide insight into the nature of the linear (one-photon) absorption bands. As a rule, the long wavelength absorption band of a single chromophore fluorene-based derivative corresponds to the single electronic transition $S_0 \rightarrow S_1$ and the values of excitation anisotropy are nearly constant in this spectral range.[20,21] As can be seen in Fig. 5a, the spectral dependences $r = f(\lambda_{ex})$ for **1** in all the investigated solvents were not constant in the long wavelength absorption band, which is indicative of two or more electronic transitions $S_0 \rightarrow S_n$ ($n = 1, 2,\ldots$) with different dipole orientations in the spectral range 360 nm $< \lambda_{ex} <$ 450 nm. Nearly constant values of r in the range 320 nm $< \lambda_{ex} <$ 360 nm with a minimum at $\approx$300 nm correspond to the spectral position of other higher energy electronic transitions of **1**. It should be mentioned that the shoulder at $\approx$300 nm (Fig. 5a, curves G and H) corresponds to the absorption of a diphenylamino moiety of **1**,[22] while the spectral position of other electronic transitions cannot be ascertained from the steady-state one-photon absorption spectrum. In low viscosity organic solvents the absolute values of r monotonically decrease with increasing τ/η (η is the viscosity of solvent), and the experimental dependence $1/r(\lambda_{ex}) = f(\tau/\eta)$ (at $\lambda_{ex} = 430$ nm) is close to a linear function (Fig. 5b).

Taking into account theoretical dependences $1/r = 1/r_0 + \tau/(r_0\theta)$ and $\theta = \eta V/kT$ (V, k, and T are the effective rotational volume of the molecule, Boltzmann constant, and absolute temperature, respectively),[12] it is possible to conclude that the fundamental anisotropy r_0 and effective rotational volume V of **1** exhibit a weak dependence on solvent properties in low viscosity organic media and the effective size of the solvate cage is close to $V \approx 11\,000$ Å^3. One can deduce from Fig. 5a, curve A, the absolute values of r in viscous pTHF ($r \approx r_0$) are far from the theoretical limit 0.4, in contrast to typical linear fluorene derivatives.[20,21] Values of anisotropy $<$0.4 in the far anti-Stokes region correspond to a relatively large angle $\alpha \sim 30°$–$35°$ (between the main absorption and emission transition dipoles of **1**), estimated from the expression: $r_0 = (3\cos^2\alpha - 1)/5$.[12] A comprehensive analysis of all linear spectral data, including space parameters of the optimized geometry, suggests possible intramolecular energy transfer between the two, nonconjugated fluorenyl chromophores in **1**. The nature of this energy transfer may be based on a non-radiative dipole–dipole Förster mechanism[12,23] and/or on intramolecular vibrational relaxation processes.[24] It should also be mentioned that two identical unconjugated chromophore systems in **1** leading to additional electronic transitions in the main one-photon absorption band can noticeably improve 2PA efficiency in this formally two-photon forbidden spectral region.

3.2 2PA properties and bioimaging

The degenerate 2PA properties of **1** were investigated by a relative 2PF method[13] under 1 kHz femtosecond excitation over a broad spectral range in solvents of different polarities (cyclohexane and DCM). The corresponding 2PA spectra are presented in Fig. 6, along with the linear absorption and excitation anisotropy spectra for convenience in analysis.

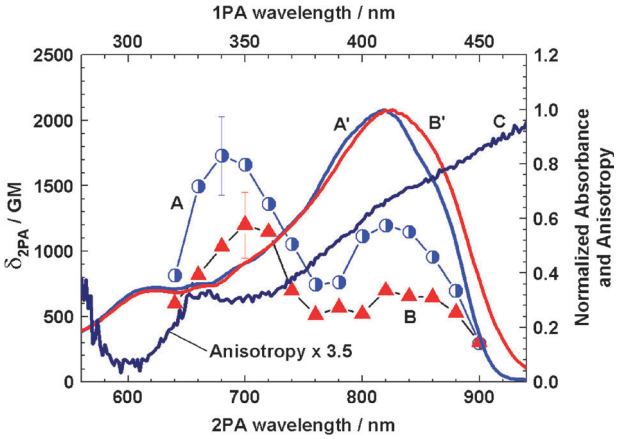

Fig. 6 2PA (A, B), normalized absorption (A′, B′), and anisotropy (C) spectra of **1** in cyclohexane (A, A′), DCM (B, B′), and pTHF (C).

The symmetrical fluorene-based structure of **1** exhibited two well defined 2PA bands at $\lambda_{ex} \approx 680$ and 820 nm with maxima cross sections $\delta_{2PA} \approx$ 1200–1700 GM and 700–1200 GM, respectively. This is in contrast to symmetrical fluorene derivatives with a single chromophore system which exhibited only one two-photon allowed short wavelength absorption band with a monotonically decreased 2PA tail in the main one-photon absorption band.[18,19,21,25] The spectral position of the short wavelength 2PA band of **1** corresponded to the shoulder at $\lambda_{ex} \approx$ 320–360 nm in the excitation anisotropy spectrum (Fig. 6, curve C) and was not apparent from the linear absorption spectra (curves A′ and B′). According to this data, the shapes of the 2PA spectra were nearly the same in the both solvents, with a noticeable decrease in the absolute values of δ_{2PA} in DCM (polar solvent). This behavior is not typical for fluorene-based derivatives and will be the subject of further investigation.

It should be mentioned that the photochemical stability of **1** under both one- and two-photon excitation was close to similar fluorene derivatives with a single chromophore system and extended π-conjugation.[26] High fluorescence quantum yields ($\Phi \approx 1.0$) and relatively large 2PA cross sections ($\delta_{2PA} \approx$ 500–1000 GM) in the main one-photon absorption band ($\sim$370–440 nm) make fluorene derivative **1** a promising candidate as a probe for two-photon bioimaging using commercial femtosecond Ti:sapphire lasers.

The use of fluorescence probe **1** as a 2PA biological contrast agent was evaluated using a HCT 116 cell line. Since probe **1** is not water soluble, a carrier system was needed. The probe was encapsulated in micelles formed by polymer Pluronic F 108NF. The images collected by DIC, one-photon fluorescence, and two-photon induced fluorescence are shown in Fig. 7 after incubating the micelle-encapsulated fluorophore with HCT 116 cells. Two-photon fluorescence was observed predominantly from the cytoplasmic region (Fig. 7B and C), consistent with images collected from conventional (one-photon) fluorescence imaging. The dye-loaded micelles appear to be selective for an organelle surrounding the nuclei, possibly the lysosomes. Typically in HCT 116 cells, the lysosomes are generally localized around the cell nucleus, consistent with what was observed in the micrographs.

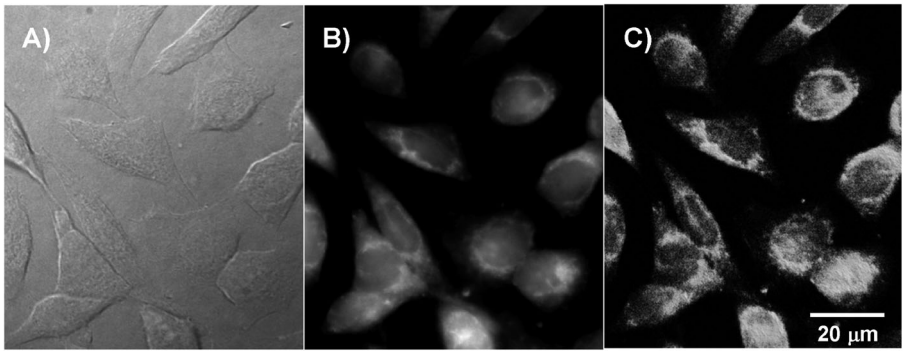

Fig. 7 Images of HCT 116 cells incubated with probe **1** (30 μM, 3 h) obtained with a 60×, oil immersion objective. (A) DIC, 400 ms. (B) One-photon fluorescence image (filter cube Ex: 377/50, DM: 409, Em: 525/40). (C) 3D reconstruction from overlaid 2PFM images (Ex: 700 nm; Em: long-pass filter 690 nm).

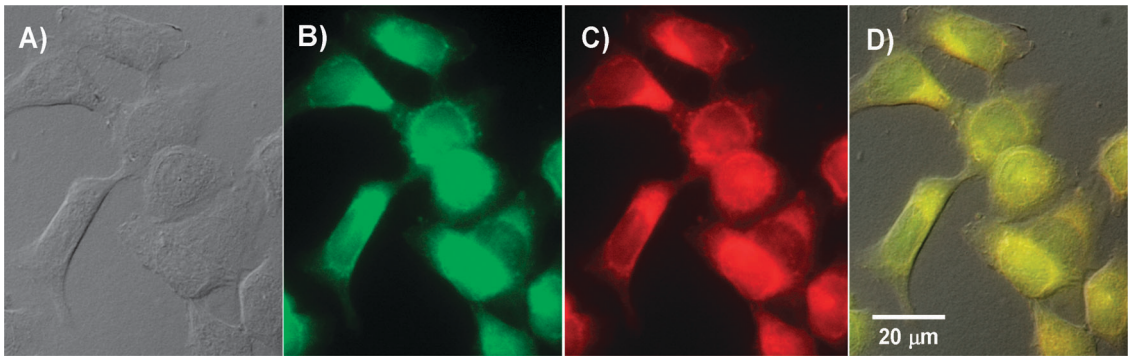

Fig. 8 Colocalization images of HCT 116 cells incubated with **1** and LysoTracker Red together, obtained with a 60×, oil immersion objective. (A) DIC, 500 ms. (B) One-photon confocal fluorescence image of **1** using a custom made filter cube (Ex: 377/50; DM: 409; Em: 525/40), 4 ms. (C) One-photon confocal fluorescence image of LysoTracker using a Texas Red filter cube (Ex: 562/40; DM: 593; Em: 624/40) 350 ms. (D) Overlapped image of A, B, and C (Pearson's correlation coefficient 0.98). The scar bar is 20 μM.

Published on 21 January 2011 on http://pubs.rsc.org | doi:10.1039/C0CP01511C
Downloaded by University of Central Florida on 17 December 2012

Subsequently, colocalization studies were conducted to ascertain the probe's organelle specificity (Fig. 8). A Pearson's correlation coefficient of 0.98 (software: Slidebook 5.0) with commercial Lysotracker Red indicates very specific labelling of the lysosomes by micelle-encapsulated probe **1**. As a stereograph is more visual than a planar view, HCT 116 cells, incubated with **1**, were scanned optical slice-by-optical slice in a confocal mode, affording 3D two-photon fluorescence images (Fig. 7C). This technique should prove useful when detailed studies of the cell phenotype are being carried out, as it will allow one to visualize small cell features relying on the intrinsic resolution of the upconverted fluorescence.

3.3 ESA and superfluorescence properties

Superfluorescence and lasing properties of fluorescent probes can, potentially, be harnessed for further improvements of the quality of microscopic imaging based on decreasing emission lifetimes and increasing spectral brightness. The optical amplification potential of **1** was investigated in polar (DCM) and nonpolar (cylcohexane) organic media in the fluorescence emission spectral range (420–750 nm). Corresponding ESA spectra were determined by pump–probe methodology[17] and presented in Fig. 9a. Potential amplification of **1** (*i.e.*, negative values of ESA) was obtained only in a nonpolar (cyclohexane)

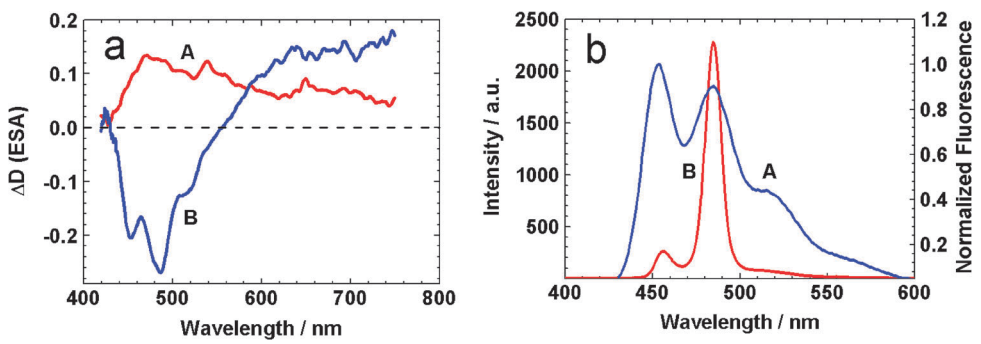

Fig. 9 (a) ESA spectra of **1** in DCM (A) and cyclohexane (B). (b) Normalized fluorescence (A) and superfluorescence (B) spectra of **1** in cyclohexane (see text for details).

 This journal is © the Owner Societies 2011

Published on 21 January 2011 on http://pubs.rsc.org | doi:10.1039/C0CP01511C
Downloaded by University of Central Florida on 17 December 2012

medium and in a restricted spectral range (~420–550 nm). In contrast, a polar (DCM) solution of **1** exhibited strong reabsorption effects in the entire fluorescence region, completely preventing amplification. An efficient superfluorescence effect under longitudinal pumping at 355 nm was observed for **1** in cyclohexane ($C \sim 10^{-4}$ M); the corresponding amplified stimulated emission spectrum is presented in Fig. 9b. The spectral width of superfluorescence spectrum was ~10 nm (FWHM) (curve B) which is much narrower than the regular fluorescence spectrum (curve 1) and close to the corresponding parameters of typical laser dyes.[27] Pluronic micelle-encapsulation provided a relatively nonpolar core to host probe **1**, suggesting potential directions for the design of amphiphilic micelle-based superfluorescent probes.

4. Conclusions

Linear photophysical, 2PA, ESA, and superfluorescence properties of new fluorenyl derivative **1** bearing two identical chromophores in its molecular structure were investigated in organic solvents and aqueous mixture as a potential fluorescent probe for two-photon fluorescence microscopy bioimaging. The steady-state absorption spectra of **1** were nearly independent of solvent polarity while no molecular aggregation effects were observed over a range of concentrations up to 2×10^{-2} M. The fluorescence spectra of symmetrical bis-fluorenyl **1** were independent of excitation wavelength in all of the investigated organic solvents and exhibited noticeable solvatochromic effects. In organic media, the fluorescence quantum yields were close to unity ($\Phi \approx 0.9$–1.0), independent of excitation wavelength over a broad spectral range, and the fluorescence emission process corresponded to a single-exponential decay. In contrast, an aqueous mixture of **1** exhibited inhomogeneous broadening of the fluorescence spectra, a noticeable decrease in fluorescence quantum yield ($\Phi \approx 0.4$), and bi-exponential fluorescence emission decay. The steady-state excitation anisotropy spectra revealed more than one electronic transition in the spectral range of the primary long wavelength absorption band of **1** and a non-parallel orientation of their transition dipole moments. A weak dependence of the fundamental anisotropy r_0 and effective rotational molecular volume V on solvent properties was shown in organic media.

The 2PA spectra of probe **1** were obtained under 1 kHz femtosecond excitation over a broad spectral range (~640–900 nm) by a relative 2PF method. 2PA efficiency was characterized by two well defined absorption bands at ≈680 and 820 nm with maximum 2PA cross sections $\delta_{2PA} \approx$ 1200–1700 GM and 500–1000 GM, respectively. The second 2PA band was relatively intense and overlapped nicely with the tuning range of commercial femtosecond Ti:sapphire lasers, an important feature for two-photon fluorescence microscopy bioimaging.

To demonstrate the potential utility of **1** as an *in vitro* probe, one- and two-photon fluorescence microscopy imaging of HCT 116 cells incubated with probe **1** encapsulated in Pluronic F 108NF was conducted. Very high specific targeting to the lysosomes was detected and confirmed by colocalization studies. 3D 2PFM imaging revealed the promising utilization of this probe for studying the subcellular organelles and activities.

The ESA spectra of **1** revealed the possibility of potential light amplification in nonpolar media. The efficient superfluorescence effect was shown for **1** in cyclohexane solution under the longitudinal pumping at 355 nm. This new superfluorescence probe is a major step in the development of a new generation of fluorescence labels with improved spectral brightness and short luminescence lifetimes. Large 2PA cross sections ($\delta_{2PA} \sim 1000$ GM), high fluorescence quantum yield ($\Phi \approx 1.0$), and good photochemical stability along with efficient superfluorescence properties make fluorenyl **1** a promising probe for 2PFM bioimaging applications with commercial Ti:sapphire lasers.

Acknowledgements

We wish to acknowledge the Civilian Research and Development Foundation (UKB2-2923-KV-07), the Ministry of Education and Science of Ukraine (grant M/49-2008), the National Institutes of Health (1 R15 EB008858-01), and the National Science Foundation (ECCS-0925712, CHE-0832622, and CHE-0840431) for partial support of this work.

References

1 S. A. Odom, S. Webster, L. A. Padilha, D. Peceli, H. Hu, G. Nootz, S. J. Chung, S. Ohira, J. D. Matichak, O. V. Przhonska, A. D. Kachkovski, S. Barlow, J. L. Bredas, H. L. Anderson, D. J. Hagan, E. W. Van Stryland and S. R. Marder, *J. Am. Chem. Soc.*, 2009, **131**, 7510–7511; X. H. Dong, Y. Y. Yang, J. Sun, Z. H. Liu and B. F. Liu, *Chem. Commun.*, 2009, 3883–3885; M. Rumi, S. J. K. Pond, T. Meyer-Friedrichsen, Q. Zhang, M. Bishop, Y. Zhang, S. Barlow, S. R. Marder and J. W. Perry, *J. Phys. Chem. C*, 2008, **112**, 8061–8071; M. Balu, L. A. Padilha, D. J. Hagan, E. W. Van Stryland, S. Yao, K. Belfield, S. J. Zheng, S. Barlow and S. Marder, *J. Opt. Soc. Am. B*, 2008, **25**, 159–165; Q. D. Zheng, G. S. He and P. N. Prasad, *Chem. Phys. Lett.*, 2009, **475**, 250–255.
2 A. Hayek, F. Bolze, J. F. Nicoud, P. L. Baldeck and Y. Mely, *Photochem. Photobiol. Sci.*, 2006, **5**, 102–106; A. R. Morales, K. J. Schafer-Hales, A. I. Marcus and K. D. Belfield, *Bioconjugate Chem.*, 2008, **19**, 2559–2567; K. J. Schafer-Hales, K. D. Belfield, S. Yao, P. K. Frederiksen, J. M. Hales and P. E. Kolattukudy, *J. Biomed. Opt.*, 2005, **10**, 051402.
3 M. Velusamy, J.-Y. Shen, J. T. Lin, Y.-C. Lin, C.-C. Hsieh, C.-H. Lai, C.-W. Lai, M.-L. Ho, Y.-C. Chen, P.-T. Chou and J.-K. Hsiao, *Adv. Funct. Mater.*, 2009, **19**, 2388–2397.
4 K. J. Schafer, J. M. Hales, M. Balu, K. D. Belfield, E. W. Van Stryland and D. J. Hagan, *J. Photochem. Photobiol., C*, 2004, **162**, 497–502.
5 K. D. Belfield and K. J. Schafer, *Chem. Mater.*, 2002, **14**, 3656–3662; C. C. Corredor, Z. L. Huang, K. D. Belfield, A. R. Morales and M. V. Bondar, *Chem. Mater.*, 2007, **19**, 5165–5173.
6 P. L. Wu, X. J. Feng, H. L. Tam, M. S. Wong and K. W. Cheah, *J. Am. Chem. Soc.*, 2009, **131**, 886–887.
7 K. A. Belfield, M. V. Bondar, F. E. Hernandez and O. V. Przhonska, *J. Phys. Chem. C*, 2008, **112**, 5618–5622.
8 S. J. Andrasik, K. D. Belfield, M. V. Bondar, F. E. Hernandez, A. R. Morales, O. V. Przhonska and S. Yao, *ChemPhysChem*, 2007, **8**, 399–404.
9 K. D. Belfield, A. R. Morales, J. M. Hales, D. J. Hagan, E. W. Van Stryland, V. M. Chapela and J. Percino, *Chem. Mater.*, 2004, **16**, 2267–2273; K. D. Belfield, A. R. Morales, B. S. Kang, J. M. Hales, D. J. Hagan, E. W. Van Stryland, V. M. Chapela and J. Percino, *Chem. Mater.*, 2004, **16**, 4634–4641; K. D. Belfield, S. Yao, J. M. Hales, M. V. Bondar, D. J. Hagan and E. W. Van Stryland, *Polym. Mater. Sci. Eng.*, 2004, **91**, 340–341.

View Article Online

10 J. P. Moreno and M. G. Kuzyk, *J. Chem. Phys.*, 2005, **123**, 194101; M. G. Kuzyk, *J. Chem. Phys.*, 2006, **125**, 154108.
11 O. S. Finikova, T. Troxler, A. Senes, W. F. DeGrado, R. M. Hochstrasser and S. A. Vinogradov, *J. Phys. Chem. A*, 2007, **111**, 6977–6990; P. A. Padmawar, J. E. Rogers, G. S. He, L. Y. Chiang, L. S. Tan, T. Canteenwala, Q. D. Zheng, J. E. Slagle, D. G. McLean, P. A. Fleitz and P. N. Prasad, *Chem. Mater.*, 2006, **18**, 4065–4074.
12 J. R. Lakowicz, *Principles of fluorescence spectroscopy*, Kluwer, New York, 1999.
13 M. A. Albota, C. Xu and W. W. Webb, *Appl. Opt.*, 1998, **37**, 7352–7356.
14 S. Yao, H. Y. Ahn, X. H. Wang, J. Fu, E. W. Van Stryland, D. J. Hagan and K. D. Belfield, *J. Org. Chem.*, 2010, **75**, 3965–3974.
15 U. Tripathy and P. B. Bisht, *J. Chem. Phys.*, 2006, **125**, 144502.
16 N. S. Makarov, M. Drobizhev and A. Rebane, *Opt. Express*, 2008, **16**, 4029–4047.
17 L. De Boni, C. Toro and F. E. Hernandez, *Opt. Express*, 2008, **16**, 957–964.
18 F. Terenziani, A. Painelli, C. Katan, M. Charlot and M. Blanchard-Desce, *J. Am. Chem. Soc.*, 2006, **128**, 15742–15755.
19 K. D. Belfield, M. V. Bondar, C. O. Yanez, F. E. Hernandez and O. V. Przhonska, *J. Mater. Chem.*, 2009, **19**, 7498–7502.
20 K. D. Belfield, M. V. Bondar, J. M. Hales, A. R. Morales, O. V. Przhonska and K. J. Schafer, *J. Fluoresc.*, 2005, **15**, 3–11; K. D. Belfield, M. V. Bondar, O. D. Kachkovsky, O. V. Przhonska and S. Yao, *J. Lumin.*, 2007, **126**, 14–20.
21 K. D. Belfield, M. V. Bondar, F. E. Hernandezt, O. V. Przhonska and S. Yao, *J. Phys. Chem. B*, 2007, **111**, 12723–12729.
22 K. D. Belfield, M. V. Bondar, I. Cohanoschi, F. E. Hernandez, O. D. Kachkovsky, O. V. Przhonska and S. Yao, *Appl. Opt.*, 2005, **44**, 7232–7238.
23 H. J. Kim, S. Y. Park, S. Yoon and J. S. Kim, *Tetrahedron*, 2008, **64**, 1294–1300.
24 S. Tobita, K. Ida and S. Shiobara, *Res. Chem. Intermed.*, 2001, **27**, 205–218.
25 L. Porres, O. Mongin, C. Katan, M. Charlot, B. K. C. Bhatthula, V. Jouikov, T. Pons, J. Mertz and M. Blanchard-Desce, *J. Nonlinear Opt. Phys. Mater.*, 2004, **13**, 451–460.
26 C. C. Corredor, K. D. Belfield, M. V. Bondar, O. V. Przhonska and S. Yao, *J. Photochem. Photobiol., A*, 2006, **184**, 105–112.
27 F. P. Shafer, *Dye Lasers*, Springer-Verlag, New York, 1973.

Published on 21 January 2011 on http://pubs.rsc.org | doi:10.1039/C0CP01511C
Downloaded by University of Central Florida on 17 December 2012

 This journal is © the Owner Societies 2011